

## Article

# Bioprospection of Tenellins Produced by the Entomopathogenic Fungus *Beauveria neobassiana*

Rita Toshe <sup>1,2</sup>, Esteban Charria-Girón <sup>1,2</sup> , Artit Khonsanit <sup>3</sup>, Janet Jennifer Luangsa-ard <sup>3</sup> ,  
Syeda Javariya Khalid <sup>1,2</sup>, Hedda Schrey <sup>1,2</sup>, Sherif S. Ebada <sup>1,4,\*</sup>  and Marc Stadler <sup>1,2,\*</sup> 

- <sup>1</sup> Department of Microbial Drugs, Helmholtz Centre for Infection Research GmbH (HZI), Inhoffenstraße 7, 38124 Braunschweig, Germany; rita.toshe@helmholtz-hzi.de (R.T.); esteban.charriagiron@helmholtz-hzi.de (E.C.-G.); syeda.khalid@helmholtz-hzi.de (S.J.K.); hedda.schrey@helmholtz-hzi.de (H.S.)
- <sup>2</sup> Institute of Microbiology, Technische Universität Braunschweig, Spielmannstraße 7, 38106 Braunschweig, Germany
- <sup>3</sup> National Center for Genetic Engineering and Biotechnology (BIOTEC), National Science and Technology Development Agency (NSTDA), 113 Thailand Science Park, Phahonyothin Rd., Khlong Nueng, Khlong Luang, Pathum Thani 12120, Thailand; artit.kho@biotec.or.th (A.K.); jafen@biotec.or.th (J.J.L.-a.)
- <sup>4</sup> Department of Pharmacognosy, Faculty of Pharmacy, Ain Shams University, Cairo 11566, Egypt
- \* Correspondence: sherif.elsayed@helmholtz-hzi.de or sherif\_elsayed@pharma.asu.edu.eg (S.S.E.); marc.stadler@helmholtz-hzi.de (M.S.); Tel.: +49-531-6181-4240 (M.S.)

**Abstract:** Fungi are known as prolific producers of bioactive secondary metabolites with applications across various fields, including infectious diseases, as well as in biological control. However, some of the well-known species are still underexplored. Our current study evaluated the production of secondary metabolites by the entomopathogenic fungus *Beauveria neobassiana* from Thailand. The fermentation of this fungus in a liquid medium, followed by preparative high-performance liquid chromatography (HPLC) purification, resulted in the isolation of a new tenellin congener, namely pretenellin C (1), together with five known derivatives (2–6). Their chemical structures were elucidated by 1D and 2D nuclear magnetic resonance (NMR) spectroscopy in combination with high-resolution electrospray ionization mass spectrometry (HR-ESI-MS). We evaluated the antimicrobial and cytotoxic activities from all isolated compounds, as well as their inhibitory properties on biofilm formation by *Staphylococcus aureus*. Generally, tenellins displayed varying antibiofilm and cytotoxic effects, allowing us to propose preliminary structure-activity relationships (SARs). Among the tested compounds, prototenellin D (2) exhibited the most prominent antibiofilm activity, while its 2-pyridone congener, tenellin (4), demonstrated potent cytotoxic activity against all tested cell lines. Given the fact that the biological activities of the tenellins have so far been neglected in the past, our study could provide a good starting point to establish more concise structure-activity relationships in the near future.

**Keywords:** Cordycipitaceae; insect fungi; biofilm inhibition; antiproliferative; SAR; PKS-NRPS



**Citation:** Toshe, R.; Charria-Girón, E.; Khonsanit, A.; Luangsa-ard, J.J.; Khalid, S.J.; Schrey, H.; Ebada, S.S.; Stadler, M. Bioprospection of Tenellins Produced by the Entomopathogenic Fungus *Beauveria neobassiana*. *J. Fungi* **2024**, *10*, 69. <https://doi.org/10.3390/jof10010069>

Academic Editor: Ming-Guang Feng

Received: 14 November 2023

Revised: 9 January 2024

Accepted: 10 January 2024

Published: 15 January 2024



**Copyright:** © 2024 by the authors. Licensee MDPI, Basel, Switzerland. This article is an open access article distributed under the terms and conditions of the Creative Commons Attribution (CC BY) license (<https://creativecommons.org/licenses/by/4.0/>).

## 1. Introduction

Fungi, renowned for their valuable contributions across a range of different fields, are also recognized for being creative secondary metabolite producers. These compounds have significantly benefited society, particularly in antibiotic development, as exemplified by the pleuromutilins, one of the most recent antibiotics class introduced to the market [1]. However, the value of these organisms extends beyond the control of infectious diseases, as fungi are instrumental in a wealth of applications, such as in agriculture, where they serve as biocontrol agents [2]. The interactions within fungal ecosystems have been leveraged to create environmentally friendly alternatives for pest control, as in the case of entomopathogenic fungi, which act against specific pests while sparing other organisms from harm [3].

Species belonging to the genus *Beauveria* (Cordycipitaceae, Ascomycota) are widely employed in agriculture as biocontrol agents [4]. Recent taxonomic revisions of this genus, facilitated by a combination of whole-genome sequencing, morphometric analysis, and chemical studies, have aided in the delimitation of the *Beauveria asiatica* and *Beauveria bassiana* (*sensu lato*) species complexes [4]. Other studies illustrated the biosynthetic potential of *Beauveria* spp. to produce diverse secondary metabolites, encompassing sesquiterpenes, steroids, tricyclic diterpenoids, cyclodepsipeptides, and various alkaloids [5,6]. Notably, compounds like beauverolides and beauvericins are known for their multifaceted roles as insecticidal, cytotoxic, and antimicrobial agents [4,7]. Similarly, the tenellins, polyketide synthase/nonribosomal-peptide synthetase (PKS-NRPS) products, originally isolated from *B. bassiana*, have been extensively studied regarding their biosynthesis [8]. However, only a limited number of studies have explored the biological functions of these secondary metabolites, and yet the full potential of these fungi remains largely untangled.

The knowledge gap extends to the complex interplay of fungal secondary metabolites and their usage in fighting the rapid increase of microbial resistance. For instance, biofilms formed by microbes often play a key role during chronic infections as they reduce the effectiveness of antibiotics, resulting in the overall increase of resistance. Nonetheless, no effective treatment for biofilm formation has been developed so far [9].

During our ongoing search for novel biofilm inhibitors, we investigated the production of secondary metabolites by the entomopathogenic fungus *B. neobassiana* from Thailand. The results are reported in the following narrative.

## 2. Materials and Methods

### 2.1. General Experimental Procedures

Optical rotations were measured at 20 °C using an MCP 150 circular polarimeter (Anton Paar, Seelze, Germany). UV/Vis spectra were collected with a Shimadzu UV2450 spectrophotometer (Shimadzu®, Kyoto, Japan). The optical rotation and UV/Vis spectra of all isolated secondary metabolites were measured in MeOH (Uvasol®, Merck, Darmstadt, Germany).

The 1D and 2D nuclear magnetic resonance (NMR) spectra of isolated compounds were obtained using an Avance III 700 spectrometer with a 5 mm TCI cryoprobe (Bruker Daltonics®, Bremen, Germany), <sup>1</sup>H NMR: 700 MHz, <sup>13</sup>C: 175 MHz, and an Avance III 500 spectrometer (Bruker, <sup>1</sup>H NMR: 500 MHz, <sup>13</sup>C: 125 MHz). Chemical shifts  $\delta$  were referenced using the solvents DMSO-*d*<sub>6</sub> or acetone-*d*<sub>6</sub>.

Analytical HPLC chromatograms and electrospray ionization mass spectra (ESI-MS) were acquired using an UltiMate 3000 Series UPLC (Thermo Fischer Scientific®, Waltham, MA, USA) equipped with a C18 column (Acquity UPLC BEH 2.1 × 50 mm, 1.7  $\mu$ m; Waters, Milford, MA, USA) and an amaZon speed ESI-Iontrap-MS (Bruker) using a sample injection volume of 2  $\mu$ L and a flow rate of 0.6 mL/min. A gradient elution was applied using a mobile phase consisting of solvent A (H<sub>2</sub>O + 0.1% formic acid (*v/v*)) and solvent B (MeCN + 0.1% formic acid (*v/v*)). The gradient started at 5% B, gradually increasing to 100% B over 20 min, followed by a 10 min hold at 100% B and UV-Vis detection in the range from 190 to 600 nm.

High-resolution electrospray ionization mass spectra (HR-ESI-MS) were obtained using an Agilent 1200 Infinity Series HPLC-UV system (Agilent Technologies®, Santa Clara, CA, USA) equipped with a C18 Acquity UPLC BEH analytical column (2.1 × 50 mm, 1.7  $\mu$ m; Waters®, Milford, MA, USA) connected to a maXis® Electrospray Time-of-flight mass spectrometer (ESI-TOF-MS; Bruker). The experimental conditions for acquiring the HR-ESI-MS data were identical to those used for ESI-MS.

### 2.2. Fungal Material

The strain *Beauveria neobassiana* Khons., Kobmoo & Luangsa-ard BCC 31604 was found growing on an adult unidentified beetle (Coleoptera) and collected and isolated on 22 July 2008, by a team including A. Khonsanit, J.J. Luangsa-ard, K. Tasanathai, P. Srikitikulchai,

and S. Mongkolsamrit. The collection site was in Chiang Rai Province, Chiang Khong District, along the scenic Phlu Kaeng Waterfall Nature Trail, located at coordinates 20.26° N latitude and 100.39° E longitude. The herbarium material and the culture of the fungus are located in the collections of BIOTEC National Science and Technology Development Agency (NSTDA), Pathum Thani, Thailand, under the designation nos. BBH 23856 (specimen) and BCC 31604 (mycelial culture), respectively. The culture represents paratype material. The complete identification and characterization of the fungus was recently reported in an integrative phylogenomic study [4], in which mostly the molecular phylogenetic data served for segregation of the new species.

### 2.3. Cultivation, Extraction and Isolation

*Beauveria neobassiana* BCC 31604 was cultured on potato dextrose agar (PDA; Fisher Scientific GmbH, Schwerte, Germany) plates for 7 days. A total of 5 mycelial plugs were carefully removed using a 7 mm diameter cork borer. The plugs were transferred into 500 mL Erlenmeyer flasks, each containing 200 mL of potato dextrose broth medium (PDB; 24 g/L; Fisher Scientific GmbH). For the main cultures, 50 flasks were used in total (10 L). The cultures were then incubated at 23 °C and 140 rpm. The glucose level was routinely monitored using urine glucose test strips (Dirui Industrial Co., Ltd., Changchun, China). The cultures were then harvested three days after the glucose was depleted. The mycelia were separated from the supernatant by vacuum filtration, and extracted separately.

A liquid–liquid extraction was conducted twice for the supernatant using ethyl acetate (1:1). The resulting organic phases were combined, filtered through anhydrous sodium sulfate, and evaporated under vacuum, while the aqueous phase was discarded. The mycelia were extracted with acetone (2 × 1 L) and subjected to two rounds of ultra-sonic bathing for 30 min at 40 °C. The resultant suspensions were filtered, and the acetone phase was collected and evaporated under vacuum. The resulting semi-solid residue from mycelial extract was then dispersed in 100 mL of water and subjected to liquid-liquid extraction against ethyl acetate as previously described. The obtained total extracts from the mycelia (91 mg) and the supernatant (269 mg) were analyzed by LC-MS and thereafter purified by preparative HPLC.

Both the mycelial and the supernatant extracts of *B. neobassiana* were subjected to purification using a PLC 2250 preparative HPLC system (Gilson, Middleton, WI, USA) and a Gemini C18 (250 × 50 mm, 10 μm; Phenomenex®, Torrance, CA, USA) as the stationary phase and the following conditions as the mobile phase: solvent A: deionized water (H<sub>2</sub>O) + 0.1% formic acid; solvent B: acetonitrile (MeCN) + 0.1% formic acid; flow: 45 mL/min for the mycelial extract and 30 mL/min for the supernatant extract; collected fraction volume: 15 mL. For the supernatant extract (269 mg), a gradient elution was applied as follows: from 35% B to 100% B in 50 min, then holding the gradient at 100% for 15 min, resulting in the isolation of five pure compounds: **6** (2.5 mg,  $t_R$  = 36 min), **5** (9.8 mg,  $t_R$  = 39 min), **2** (7.5 mg,  $t_R$  = 48 min), **3** (1.5 mg,  $t_R$  = 57 min), and **4** (4.0 mg,  $t_R$  = 60 min). For the mycelial extract (91 mg), gradient elution was applied as follows: from 25% B to 100% B in 65 min and ended with isocratic elution at 100% for 10 min, affording three pure substances: **1** (1.2 mg,  $t_R$  = 41 min), **6** (1.2 mg,  $t_R$  = 51 min), and **5** (1.8 mg,  $t_R$  = 54 min).

### 2.4. Spectral Data

#### 2.4.1. Pretenellin C (**1**)

Yellow amorphous solid; UV/Vis (MeOH)  $\lambda_{max}$  (log  $\epsilon$ ) 332 nm (3.86), 249 nm (4.40), 200 nm (4.58); NMR data (<sup>1</sup>H: 500 MHz, <sup>13</sup>C: 125 MHz, acetone-*d*<sub>6</sub>) see Table 1; HR-ESI-MS:  $m/z$  246.0393 [M–H<sub>2</sub>O+H]<sup>+</sup> (calcd. 246.0397 for C<sub>12</sub>H<sub>8</sub>NO<sub>5</sub><sup>+</sup>), 264.0499 [M+H]<sup>+</sup> (calcd. 264.0503 for C<sub>12</sub>H<sub>10</sub>NO<sub>6</sub><sup>+</sup>).

#### 2.4.2. Prototenellin D (**2**)

Pale yellow amorphous solid;  $[\alpha]_D^{20}$  –264° (c 0.01, MeOH); UV/Vis (MeOH)  $\lambda_{max}$  (log  $\epsilon$ ) 368 nm, 224 nm, 200 nm; NMR data (<sup>1</sup>H: 500 MHz, <sup>13</sup>C: 125 MHz, DMSO-*d*<sub>6</sub>) comparable to

the previously described spectral data [8]; HR-ESI-MS:  $m/z$  354.1707 [M–H<sub>2</sub>O+H]<sup>+</sup> (calcd. 354.1700 for C<sub>21</sub>H<sub>24</sub>NO<sub>4</sub><sup>+</sup>), 372.1812 [M+H]<sup>+</sup> (calcd. 372.1805 for C<sub>21</sub>H<sub>26</sub>NO<sub>5</sub><sup>+</sup>), 394.1633 [M+Na]<sup>+</sup> (calcd. 394.1625 for C<sub>21</sub>H<sub>25</sub>NNaO<sub>5</sub><sup>+</sup>).

#### 2.4.3. Pretenellin B (3)

Bright yellow powder; UV/Vis (MeOH)  $\lambda_{\max}$  (log  $\epsilon$ ) 346 nm, 230 nm; NMR data (<sup>1</sup>H: 500 MHz, <sup>13</sup>C: 125 MHz, DMSO-*d*<sub>6</sub>) comparable to the previously described spectral data [8]; HR-ESI-MS:  $m/z$  354.1700 [M+H]<sup>+</sup> (calcd. 354.1700 for C<sub>21</sub>H<sub>24</sub>NO<sub>4</sub><sup>+</sup>), 376.1521 [M+Na]<sup>+</sup> (calcd. 376.1519 for C<sub>21</sub>H<sub>23</sub>NNaO<sub>4</sub><sup>+</sup>).

#### 2.4.4. Tenellin (4)

Yellow solid powder; UV/Vis (MeOH)  $\lambda_{\max}$  (log  $\epsilon$ ) 344 nm, 221 nm; NMR data (<sup>1</sup>H: 500 MHz) comparable to the previously described spectral data [8]; HR-ESI-MS:  $m/z$  352.1550 [M–H<sub>2</sub>O+H]<sup>+</sup> (calcd. 352.1543 for C<sub>21</sub>H<sub>22</sub>NO<sub>4</sub><sup>+</sup>), 370.1656 [M+H]<sup>+</sup> (calcd. 370.1649 for C<sub>21</sub>H<sub>24</sub>NO<sub>5</sub><sup>+</sup>), 392.1477 [M+Na]<sup>+</sup> (calcd. 392.1468 for C<sub>21</sub>H<sub>23</sub>NNaO<sub>5</sub><sup>+</sup>).

#### 2.4.5. 15-Hydroxytenellin (5)

Yellow amorphous solid; UV/Vis (MeOH)  $\lambda_{\max}$  (log  $\epsilon$ ) 344 nm, 250 nm, 210 nm; NMR data (<sup>1</sup>H: 500 MHz, <sup>13</sup>C: 125 MHz, DMSO-*d*<sub>6</sub>) comparable to the previously described spectral data [8]; HR-ESI-MS:  $m/z$  368.1490 [M–H<sub>2</sub>O+H]<sup>+</sup> (calcd. 368.1492 for C<sub>21</sub>H<sub>22</sub>NO<sub>5</sub><sup>+</sup>), 386.1598 [M+H]<sup>+</sup> (calcd. 386.1598 for C<sub>21</sub>H<sub>24</sub>NO<sub>6</sub><sup>+</sup>), 408.1416 [M+Na]<sup>+</sup> (calcd. 408.1418 for C<sub>21</sub>H<sub>23</sub>NNaO<sub>6</sub><sup>+</sup>).

#### 2.4.6. Pyridovericin (6)

Yellow oil; UV/Vis (MeOH)  $\lambda_{\max}$  (log  $\epsilon$ ) 342 nm, 248 nm, 210 nm; NMR data (<sup>1</sup>H: 500 MHz, <sup>13</sup>C: 125 MHz, DMSO-*d*<sub>6</sub>) comparable to the previously described spectral data [10]; HR-ESI-MS:  $m/z$  352.1541 [M–H<sub>2</sub>O+H]<sup>+</sup> (calcd. 352.1543 for C<sub>21</sub>H<sub>22</sub>NO<sub>4</sub><sup>+</sup>), 370.1649 [M+H]<sup>+</sup> (calcd. 370.1649 for C<sub>21</sub>H<sub>24</sub>NO<sub>5</sub><sup>+</sup>), 392.1467 [M+Na]<sup>+</sup> (calcd. 392.1468 for C<sub>21</sub>H<sub>23</sub>NNaO<sub>5</sub><sup>+</sup>).

### 2.5. Biological Assays

All isolated compounds were assessed for their antimicrobial activity using a serial dilution assay over a concentration range from 67 to 0.5  $\mu\text{g}/\text{mL}$  following the previously described protocols [11,12]. In brief, the antimicrobial activity of all isolated metabolites was assessed by determining their minimum inhibitory concentration (MIC) against a range of different pathogens, including five fungal species: *Candida albicans* [DSM 1665], *Mucor hiemalis* [DSM 2656], *Schizosaccharomyces pombe* [DSM 70572], *Rhodotorula glutinis* [DSM 10134], and *Wickerhamomyces anomalus* [DSM 6766], as well as various Gram-positive: *Staphylococcus aureus* [DSM 346], *Bacillus subtilis* [DSM 10], *Mycolicibacterium smegmatis* [ATCC 700084], and Gram-negative bacteria: *Acinetobacter baumannii* [DSM 30008], *Escherichia coli* [DSM 1116], *Chromobacterium violaceum* [DSM 30191], and *Pseudomonas aeruginosa* [PA14]. In our experiments, gentamicin served as the positive control against most bacteria, while nystatin acted as the positive control against all fungi. For specific microorganisms, namely *A. baumannii*, *B. subtilis*, and *M. smegmatis*, ciprofloxacin, oxytetracycline, and kanamycin were used as positive controls, respectively.

The cytotoxicity of isolated compounds was determined as previously described [11,12] over a concentration range between 1 and 37  $\mu\text{g}/\text{mL}$  against two mammalian cell lines: mouse fibroblasts (L-929) and human endocervical adenocarcinoma (KB-3.1). For compounds that exhibited cytotoxic properties against the first two cell lines, we also evaluated their cytotoxicity against breast cancer (MCF-7) and lung cancer (A-549) cell lines. Epothilone B served as the positive control. Following 5 days of incubation, we determined the minimum concentration of the tested compounds required to achieve 50% growth inhibition, expressed as IC<sub>50</sub> values.

The compounds were evaluated for their ability to inhibit *S. aureus* (DSM 1104) biofilm formation, following the established procedure [13]. Briefly, serially diluted compounds (125–7.8  $\mu\text{g}/\text{mL}$ ) were co-incubated with *S. aureus* in 96-well plates in CASO medium supplemented with 4% of glucose (see Supplementary Materials). Biofilm inhibition was assessed by using Crystal Violet staining after 21 h, with microporenic acid A serving as a positive control and methanol as solvent control [14].

### 3. Results

#### 3.1. Isolation and Structure Elucidation of Secondary Metabolites

Six secondary metabolites (1–6) were isolated after the scaled-up fermentation of *B. neobassiana* in PDB medium and subsequent purification of the obtained total extracts. As can be seen in Figure 1, the composition of the mycelial and culture filtrate extracts was similar, but the more lipophilic components 3 and 4 were preferentially located in the mycelial extracts. To establish their chemical structures, each of these compounds was analyzed using HR-ESI-MS, 1D- and 2D-NMR spectroscopy.

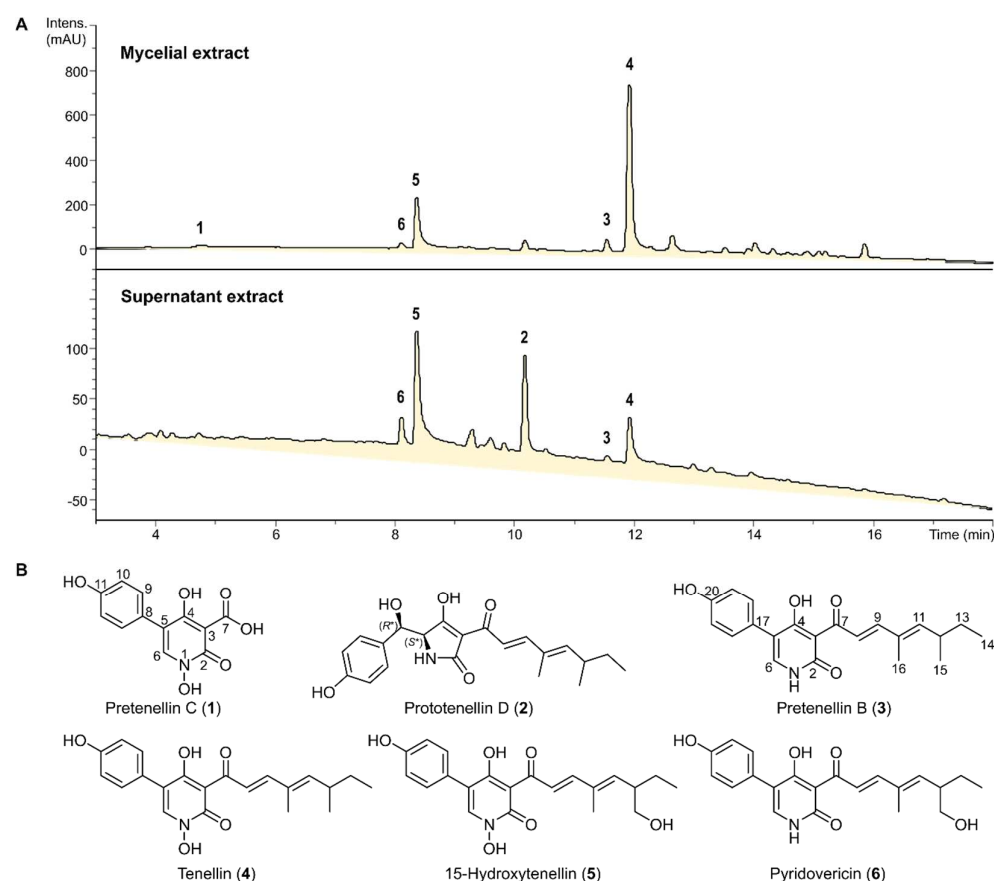


**Figure 1.** (A) HPLC–UV/Vis chromatograms (210 nm) of the crude extracts obtained from the mycelia and supernatant from the scaled-up fermentation of *B. neobassiana* in PDB medium. (B) Chemical structures of the isolated metabolites 1–6.

Compound 1 was obtained as a yellow amorphous solid, and its molecular formula was established as  $\text{C}_{12}\text{H}_9\text{NO}_6$  indicating nine degrees of unsaturation based on the HR-ESI-MS spectrum (Figure S2) revealing a protonated molecule at  $m/z$  264.0499  $[\text{M}+\text{H}]^+$  (calculated 264.0503). The  $^1\text{H}$  NMR spectrum of 1 (Table 1, Figure S3) revealed the presence of two proton resonances at  $\delta_{\text{H}}$  7.42 and  $\delta_{\text{H}}$  6.92, each with an integration index of 2, and both appeared as a doublet peak with an identical coupling constant ( $J$  value) of 8.3 Hz, indicating that compound 1 comprises a *para*-disubstituted aromatic ring. In addition, 1 also revealed two more deshielded singlet proton peaks at  $\delta_{\text{H}}$  8.18 directly correlated via

the HSQC spectrum (Figure S6) to a deshielded olefinic carbon at  $\delta_C$  138.7, suggesting its presence in a heterocyclic aromatic ring and a second broad peak at  $\delta_H$  13.90 suggesting that **1** might comprise in its structure a carboxylic acid moiety.

By comparing the obtained results with the reported literature, compound **1** was tentatively identified as a 2-pyridone derivative [8]. To further confirm the depicted structure of **1**, its HMBC spectrum (Figures 2 and S5) revealed key correlations from the deshielded aromatic proton at  $\delta_H$  8.18 (H-6) to four aromatic carbons distinguished into a carbonyl carbon ( $\delta_C$  161.2), an oxygenated aromatic carbon ( $\delta_C$  170.5), and two other unprotonated carbons ( $\delta_C$  123.6 and  $\delta_C$  115.3) that were assigned to C-2, C-4, C-5, and C-8, respectively. The HMBC spectrum of **1** (Figures 2 and S5) revealed key correlations from two electromagnetically equivalent aromatic protons at  $\delta_H$  7.42 (d,  $J = 8.3$  Hz, H-9/H-13) to a carbon resonance at  $\delta_C$  123.6 (C-4), confirming the presence of the phenyl moiety at C-4 of the 2-pyridone ring. By comparing the obtained  $^1H$  and  $^{13}C$  NMR data of **1** (Table 1) to those obtained and reported for pretenellin B (**3**) and 15-hydroxytenellin (**5**) [8], compound **1** was confirmed to feature N-OH and 3-carboxylic acid groups in its structure and hence to be a previously undescribed tenellin derivative that was trivially named as pretenellin C.

**Table 1.**  $^1H$  and  $^{13}C$  NMR data of **1**.

pos.	$\delta_H$ <sup>a</sup> (multi, $J$ [Hz])	$\delta_C$ , <sup>b</sup> Type
2		161.2, CO
3		98.2, C
4		170.5, CO
5		123.6, C
6	8.18 (s, 1H)	138.7, CH
7	13.94 (br)	n.d. <sup>c</sup>
8		115.3, C
9,13	7.42 (d, 8.3, 2H)	131.2, CH
10,12	6.92 (d, 8.3, 2H)	115.9, CH
11		158.4, C

<sup>a</sup> Measured in DMSO- $d_6$  at 500 MHz. <sup>b</sup> Assigned based on HMBC and HSQC spectra. <sup>c</sup> n.d.: Not determined.

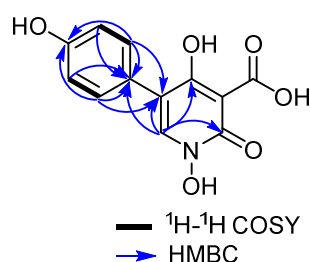


**Figure 2.** Key  $^1H$ - $^1H$  COSY and HMBC correlations of **1**.

### 3.2. Biological Effects of Tenellin-Derived Metabolites

All isolated compounds were examined for their cytotoxic activity against two cell lines, L929 (fibroblast) and KB3.1 (ovary). The obtained results (Table 2) revealed that tenellin (**4**) was an equi- and the most potent against both cell lines with  $IC_{50}$  values of 0.79  $\mu M$ . In addition, 15-hydroxytenellin (**5**) and pyridovericin (**6**) exhibited less potent cytotoxic activities against the same cell lines with  $IC_{50}$  values ranging from 4.9 to 6.8  $\mu M$ , while pretenellin C (**1**), prototenellin D (**2**) and pretenellin B (**3**) showed weak or no activity. Compounds **4–6** were further assessed against two additional cell lines namely, A-549 (lung) and MCF-7 (breast), where tenellin kept its leading potency with  $IC_{50}$  values of 0.24 and 2.0  $\mu M$ , respectively, compared to epothilone B, a microtubule stabilizer first

reported from the myxobacterium *Sorangium cellulosum* [15] and exhibited cytotoxic activity in paclitaxel-resistant tumor models [16]. Therefore, tenellin (4) with IC<sub>50</sub> values down to low micromolar or nanomolar ranges could be noted as a promising scaffold to derivatize for developing a hit molecule for a cytotoxic lead compound.

**Table 2.** Cytotoxicity (IC<sub>50</sub>) of compounds 1–6.

Test Cell Line	IC <sub>50</sub> (μM)						Positive Control
	1	2	3	4	5	6	Epothilone B (nM)
L929 (fibroblast)	n.a.	70.1	48.2	0.79	6.8	5.7	0.65
KB3.1 (ovary)	n.a.	64.7	20.2	0.79	6.0	4.9	0.17
A549 (lung)	n.d.	n.d.	n.d.	0.24	2.6	24.1	0.05
MCF-7 (breast)	n.d.	n.d.	n.d.	2.0	8.1	7.3	0.07

n.d.: not determined, n.a.: no effects up to 37 μg/mL.

All the isolated compounds were assessed for their antimicrobial activity against a panel of twelve microorganisms including Gram positive, Gram negative bacterial and fungal strains. The obtained results (Table 3) revealed that compounds 3–6 featured moderate to potent activities in particular against *S. aureus* and *B. subtilis* with tenellin (4) recognized as the most active at MIC values of 16.6 and 8.3 μg/mL, respectively.

**Table 3.** Minimum inhibitory concentration (MIC, μg/mL) of 1–6 against test organisms.

Test Microorganism	MIC (μg/mL)						Positive Control
	1	2	3	4	5	6	(μg/mL)
<i>Staphylococcus aureus</i>	n.i.	n.i.	66.6	16.6	66.6	66.6	0.21 <sup>G</sup>
<i>Escherichia coli</i>	n.i.	n.i.	n.i.	n.i.	n.i.	n.i.	0.42 <sup>G</sup>
<i>Bacillus subtilis</i>	n.i.	n.i.	66.6	8.3	66.6	66.6	16.6 <sup>O</sup>
<i>Pseudomonas aeruginosa</i>	n.i.	n.i.	n.i.	n.i.	n.i.	n.i.	0.21 <sup>G</sup>
<i>Wickerhamomyces anomalus</i>	n.d.	n.i.	n.d.	n.i.	n.i.	n.d.	16.6 <sup>N</sup>
<i>Candida albicans</i>	n.i.	n.i.	n.i.	66.6	n.i.	n.i.	8.3 <sup>N</sup>
<i>Acinetobacter baumannii</i>	n.d.	n.i.	n.d.	n.i.	n.i.	n.d.	0.52 <sup>C</sup>
<i>Chromobacterium violaceum</i>	n.d.	n.i.	n.i.	n.i.	n.i.	n.d.	1.70 <sup>G</sup>
<i>Schizosaccharomyces pombe</i>	n.d.	n.i.	n.d.	n.i.	n.i.	n.d.	4.20 <sup>N</sup>
<i>Mucor hiemalis</i>	n.i.	n.i.	n.i.	66.6	n.i.	n.i.	8.30 <sup>N</sup>
<i>Rhodotorula glutinis</i>	n.d.	n.i.	n.d.	n.i.	n.i.	n.d.	4.20 <sup>N</sup>
<i>Mycobacterium smegmatis</i>	n.i.	n.i.	n.i.	n.i.	n.i.	n.i.	1.70 <sup>K</sup>

n.i.: no inhibition up to 67 μg/mL. n.d.: not determined. G: Gentamycin; O: Oxytetracycline; N: Nystatin; C: Ciprofloxacin; K: Kanamycin.

Furthermore, compounds 1–6 were evaluated for their antibiofilm properties against the pathogenic bacterium *S. aureus*. All tested compounds exhibited moderate inhibitory activities towards *S. aureus* (Figure 3, Table S1), with prototenellin D (2) being the most effective one. It inhibited the formation of *S. aureus* biofilms for more than 50% up to a concentration of 7.8 μg/mL. However, biofilm inhibition of pretenellin B (3) and tenellin (4) were also quite notable with activities of ca. 30% lasting till concentration of 7.8 μg/mL. Pretenellin C (1) and pyridovericin (6) were least active with activity loss below concentrations of 31.3 μg/mL and 62.5 μg/mL (Table S1), respectively.

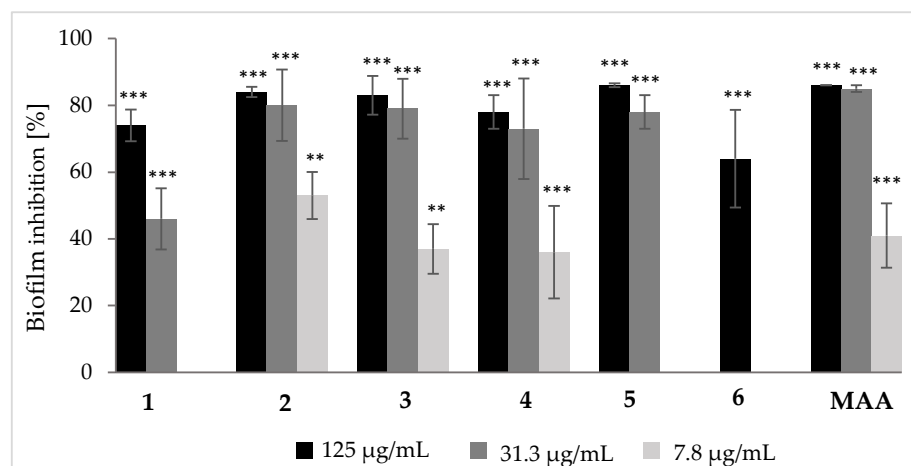


**Figure 3.** Inhibitory activity of compounds 1–6 and microporenic acid (MAA, positive control) on biofilm formation of *S. aureus* compared to the solvent control (MeOH, 0% biofilm inhibition). Error bars indicate SD of triplicates;  $p$  values: \*\*  $p < 0.01$ , \*\*\*  $p < 0.001$ . Differences between samples and the control group were determined by a two-tailed Student's  $t$ -test. Statistical significance was defined as  $p < 0.01$ .

#### 4. Discussion

Secondary metabolites featuring the 2-pyridone moiety are previously reported from different sources with a wide range of biological activities as exemplified by furanopyridones [17], aspyridones [18] and ricinine [19]. Tenellins, 2-pyridone-containing compounds previously reported from *Beauveria bassiana* [8,10], have served as model compounds for investigating the biosynthesis of fungal metabolites. Exploring their biosynthetic pathway unveiled their respective biosynthetic gene clusters (BGCs) [8]. Remarkably, similar metabolites have been shown to exhibit a broad range of bioactivities including prominent neuritogenic and cytotoxic activities [20] in addition to their antimicrobial and antimalarial properties [21].

Herein, six tenellin derivatives were obtained from *B. neobassiana* distinguished into five known (2–6) alongside with one previously undescribed derivative, pretenellin C (1) whose closely related derivative, lacking the hydroxyl group at C-11, was patented in 2004 as an antiviral agent against hepatitis C virus [22].

In the cytotoxicity assay, tenellin (4) was the most potent suggesting a plausible role for both the 2-pyridone moiety and the aliphatic side chain in comparison to pretenellin C (1) and prototenellin D (3), respectively. The aliphatic side chain may impart higher lipophilicity, thus facilitating cell wall penetration. This notion was further supported by the observed 2- to 10-fold reduction in  $IC_{50}$  values for 5 and 6 compared to 4, both featured an additional hydroxyl group at C-15 that might hinder cell penetration by raising the side chain polarity. On the contrary, pretenellin C (1) and prototenellin D (2), lacking the aliphatic side chain or 2-pyridone moiety, respectively, displayed no cytotoxicity that further supports the proposed structure-activity relationships. Intriguingly, the presence of N-hydroxylation, in 4 and 5 compared to 6, did not reveal a notable influence on their cytotoxic effects.

In the antimicrobial activity assay, only compounds 3–6 revealed antimicrobial effects with tenellin (4) as the most active against *B. subtilis* and *S. aureus* at MICs of 8.3 and 16.6 µg/mL, respectively. Similarly, tenellin was reported in literature to possess antimicrobial activity against *S. aureus* (MIC = 6.25 µg/mL) and *Curvularia lunata* (MIC = 3.13 µg/mL) [21]. Compounds 3, 5 and 6 revealed comparable activities against both tested microorganisms with MIC values of 66.6 µg/mL. By comparing their structures, it can be presumably deduced that N-hydroxylation of the 2-pyridone moiety in 4 resulted in a 4- to 8-fold increase in its antibacterial potency compared to 3 while the hydroxylation

at C-15 as in **5** reduced antimicrobial activities against the same microorganisms and getting MIC values back to 66.6 µg/mL.

In the biofilm inhibitory assay against *S. aureus*, prototenellin D (**2**), pretenellin B (**3**) and tenellin (**4**) revealed promising activities in a dose-dependent manner. However, the results obtained with 2-pyridone derivatives revealed that the aliphatic side chain at C-3 potentiates antibiofilm activity as demonstrated by tenellin (**4**) compared to pretenellin C (**1**). On the contrary, the hydroxylation at C-15 on of the side chain as in 15-hydroxytenellin (**5**), rather than tenellin (**4**), negatively affected the biofilm inhibitory activity over the tested concentration range.

In conclusion, this study reports the results of chemical and biological prospection of tenellin derivatives from the entomopathogenic fungus *B. neobassiana*. The interpretation of these results suggested some preliminary structure-activity relationships (SARs) that might be useful for future development of antibiofilm agents, which in turn could be an alternative strategy to overcome multi-drug resistant human pathogens. Notably, for the biofilm inhibitors, the final goal could be to use them in combination with established antibiotics, in order to potentiate their activity because many antibiotics are not efficient enough when exposed to microbial biofilms. Future studies on this phenomenon may be rewarding. However, given the facts that (i) our present study is the first where a significant number of compounds have been tested simultaneously and (ii) it will most probably be necessary to employ semi-synthesis based on the availability of the tenellins in gram amounts, this would go far beyond the scope of the current work.

**Supplementary Materials:** The following supporting information can be downloaded at: <https://www.mdpi.com/article/10.3390/jof10010069/s1>, Figures S1–S35: HPLC chromatograms, LR-/HR-ESI-MS and 1D/2D NMR spectra of **1–6** in acetone-*d*<sub>6</sub> or DMSO-*d*<sub>6</sub> at 500 (for <sup>1</sup>H) and 125 (for <sup>13</sup>C) MHz. Table S1. Inhibition of biofilm formation of *S. aureus* by compounds **1–6** at different concentrations.

**Author Contributions:** Conceptualization: R.T., S.S.E. and M.S.; fungal isolation and identification: A.K., J.J.L.-a.; methodology: R.T., E.C.-G. and S.S.E.; formal analysis: R.T. and E.C.-G.; data curation and structure elucidation: S.S.E.; antibiofilm assay: H.S. and S.J.K.; writing—original draft preparation: R.T., E.C.-G. and S.S.E.; writing—review and editing: S.S.E. and M.S.; project administration: J.J.L.-a. and M.S.; funding acquisition, M.S. All authors have read and agreed to the published version of the manuscript.

**Funding:** This research benefited from the European Union’s H2020 Research and Innovation Staff Exchange program (MSCA-RISE grant no. 101008129, Acronym: MYCOBIOMICS) and from the Southeast Asia-Europe Joint Funding Scheme (SEA-Europe Grant number JFS20ST-127, Acronym: Antiviralfun). S.J.K. acknowledges the German Academic Exchange Service (DAAD) for supporting her through a doctoral stipend number 91726436. The Alexander von Humboldt (AvH) Foundation is gratefully acknowledged for granting S.S.E. the Georg-Forster Fellowship for Experienced Researchers stipend (Ref 3.4-1222288-EGY-GF-E). E.C.-G. was supported by the HZI POF IV Cooperativity and Creativity Project Call. R.T. is grateful for a grant from “Die Bischöfliche Studienförderung Cusanuswerk”.

**Institutional Review Board Statement:** Not applicable.

**Informed Consent Statement:** Not applicable.

**Data Availability Statement:** The DNA sequences are deposited in GenBank (<https://www.ncbi.nlm.nih.gov/genbank/>) and all other relevant data are included in the Supplementary Information.

**Acknowledgments:** The authors acknowledge Wera Collisi for assistance with the bioassays, Kirsten Harmrolfs and Esther Surges for conducting the NMR spectroscopic measurements, as well as Aileen Gollasch for running the HR-ESI-MS analyses.

**Conflicts of Interest:** The authors declare no conflicts of interest.

## References

1. Mapook, A.; Hyde, K.D.; Hassan, K.; Kemkuignou, B.M.; Čmoková, A.; Surup, F.; Kuhnert, E.; Paomephan, P.; Cheng, T.; de Hoog, S.; et al. Ten decadal advances in fungal biology leading towards human well-being. *Fungal Divers.* **2022**, *116*, 547–614. [[CrossRef](#)]
2. Niego, G.A.T.; Lambert, C.; Mortimer, P.; Thongklang, N.; Rapior, S.; Grosse, M.; Schrey, H.; Charria-Girón, E.; Hyde, K.D.; Stadler, M. The contribution of fungi to the global economy. *Fungal Divers.* **2023**, *121*, 95–137. [[CrossRef](#)]
3. Mongkolsamrit, S.; Khonsanit, A.; Thanakitpipattana, D.; Tasanathai, K.; Noisripoom, W.; Lamlerththon, S.; Himaman, W.; Houbraken, J.; Samson, R.A.; Luangsa-ard, J. Revisiting *Metarhizium* and the description of new species from Thailand. *Stud. Mycol.* **2020**, *95*, 171–251. [[CrossRef](#)] [[PubMed](#)]
4. Kobmoo, N.; Arnarnart, N.; Pootakham, W.; Sonthirod, C.; Khonsanit, A.; Kuephadungphan, W.; Suntivich, R.; Mosunova, O.V.; Giraud, T.; Luangsa-ard, J.J. The integrative taxonomy of *Beauveria asiatica* and *B. bassiana* species complexes with whole-genome sequencing, morphometric and chemical analyses. *Persoonia* **2021**, *47*, 136–150. [[CrossRef](#)] [[PubMed](#)]
5. Du, F.Y.; Li, X.M.; Sun, Z.C.; Meng, L.H.; Wang, B.G. Secondary metabolites with agricultural antagonistic potentials from *Beauveria felina*, a marine-derived entomopathogenic fungus. *J. Agric. Food Chem.* **2020**, *68*, 14824–14831. [[CrossRef](#)]
6. Buchanan, G.O.; Williams, L.A.; Reese, P.B. Biotransformation of cadinane sesquiterpenes by *Beauveria bassiana* ATCC 7159. *Phytochemistry* **2000**, *54*, 39–45. [[CrossRef](#)]
7. Wang, H.; Peng, H.; Li, W.; Cheng, P.; Gong, M. The toxins of *Beauveria bassiana* and the strategies to improve their virulence to insects. *Front. Microbiol.* **2021**, *12*, 705343. [[CrossRef](#)] [[PubMed](#)]
8. Halo, L.M.; Heneghan, M.N.; Yakasai, A.A.; Song, Z.; Williams, K.; Bailey, A.M.; Cox, R.J.; Lazarus, C.M.; Simpson, T.J. Late stage oxidations during the biosynthesis of the 2-pyridone tenellin in the entomopathogenic fungus *Beauveria bassiana*. *J. Am. Chem. Soc.* **2008**, *130*, 17988–17996. [[CrossRef](#)]
9. Mirghani, R.; Saba, T.; Khaliq, H.; Mitchell, J.; Do, L.; Chambi, L.; Diaz, K.; Kennedy, T.; Alkassab, K.; Huynh, T.; et al. Biofilms: Formation, drug resistance and alternatives to conventional approaches. *AIMS Microbiol.* **2022**, *8*, 239–277. [[CrossRef](#)]
10. Takahashi, S.; Kakinuma, N.; Uchida, K.; Hashimoto, R.; Yanagisawa, T.; Nakagawa, A. Pyridovericin and pyridomacrolidin: Novel metabolites from entomopathogenic fungi *Beauveria bassiana*. *J. Antibiot.* **1998**, *51*, 596–598. [[CrossRef](#)]
11. Becker, K.; Wessel, A.-C.; Luangsa-ard, J.J.; Stadler, M. Viridistratins A-C, antimicrobial and cytotoxic benzo[*j*]fluoranthrenes from stomata of *Annulohyphoxylon viridistatum* (Hypoxylaceae, Ascomycota). *Biomolecules* **2020**, *10*, 805. [[CrossRef](#)] [[PubMed](#)]
12. Charria-Girón, E.; Stchigel, A.M.; Čmoková, A.; Kolařík, M.; Surup, F.; Marin-Felix, Y. *Amesia hispanica* sp. nov., producer of the antifungal class of antibiotics dactylfungins. *J. Fungi* **2023**, *9*, 463. [[CrossRef](#)] [[PubMed](#)]
13. Soliga, K.J.; Bär, S.I.; Oberhuber, N.; Zeng, H.; Schrey, H.; Schobert, R. Synthesis and bioactivity of ancorinoside B, a marine diglycosyl tetramic acid. *Mar. Drugs* **2021**, *19*, 583. [[CrossRef](#)] [[PubMed](#)]
14. Chepkirui, C.; Yuyama, K.T.; Wanga, L.A.; Decock, C.; Matasyoh, J.C.; Abraham, W.-R.; Stadler, M. Microporenic acids A-G, biofilm inhibitors, and antimicrobial agents from the basidiomycete *Microporus* Species. *J. Nat. Prod.* **2018**, *81*, 778–784. [[CrossRef](#)]
15. Gerth, K.; Bedorf, N.; Höfle, G.; Irschik, H.; Reichenbach, H. Epothilones A and B: Antifungal and cytotoxic compounds from *Sorangium cellulosum* (Myxobacteria): Production, physico-chemical and biological properties. *J. Antibiot.* **1996**, *49*, 560–563. [[CrossRef](#)]
16. Goodin, S.; Kane, M.P.; Rubin, E.H. Epothilones: Mechanism of action and biologic activity. *J. Clin. Oncol.* **2004**, *22*, 2015–2025. [[CrossRef](#)]
17. Yin, Y.; Wang, D.; Wu, D.; He, W.; Zuo, M.; Zhu, W.; Xu, Y.; Wang, L. Two New 4-Hydroxy-2-pyridone Alkaloids with antimicrobial and cytotoxic activities from *Arthrinium* sp. GZWMJZ-606 endophytic with *Houttuynia cordata* Thunb. *Molecules* **2023**, *28*, 2192. [[CrossRef](#)]
18. Bergmann, S.; Schumann, J.; Scherlach, K.; Lange, C.; Brakhage, A.A. Genomics-driven discovery of PKS-NRPS hybrid metabolites from *Aspergillus nidulans*. *Nat. Chem. Biol.* **2007**, *3*, 213–217. [[CrossRef](#)]
19. Rizwan-ul-Haq, M.; Hu, Q.B.; Hu, M.Y.; Lin, Q.S.; Zhang, W.L. Biological impact of harmaline, ricinine and their combined effects with *Bacillus thuringiensis* on *Spodoptera exigua* (Lepidoptera: Noctuidae). *J. Pest Sci.* **2009**, *82*, 327–334. [[CrossRef](#)]
20. Schmidt, K.; Riese, U.; Li, Z.; Hamburger, M. Novel tetramic acids and pyridone alkaloids, militarinones B, C, and D, from the insect pathogenic fungus *Paecilomyces militaris*. *J. Nat. Prod.* **2003**, *66*, 378–383. [[CrossRef](#)]
21. Kornsakulkarn, J.; Pruksatrakul, T.; Surawatanawong, P.; Thangsriekattigun, C.; Komwijit, S.; Boonyuen, N.; Thongpanchang, C. Antimicrobial, antimalarial, and cytotoxic substances from the insect pathogenic fungus *Beauveria asiatica* BCC 16812. *Phytochem. Lett.* **2021**, *43*, 8–15. [[CrossRef](#)]
22. Colarusso, S.; Narjes, F. Preparation of Pyridine N-oxides as Antiviral Agents. WO2004110442 A1, 23 December 2004.

**Disclaimer/Publisher’s Note:** The statements, opinions and data contained in all publications are solely those of the individual author(s) and contributor(s) and not of MDPI and/or the editor(s). MDPI and/or the editor(s) disclaim responsibility for any injury to people or property resulting from any ideas, methods, instructions or products referred to in the content.